

# Influence of the Type of Surfactant on the Formation of Calcium Phosphate in Organized Molecular Systems

S. Sarda, M. Heughebaert, and A. Lebugle\*

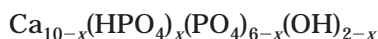
Laboratoire de Physico-chimie des Phosphates, INPT-ENSCT, CNRS-UPRESA 5071,  
38 Rue des 36 Ponts, 31400 Toulouse

Received February 24, 1999. Revised Manuscript Received May 27, 1999

Organized molecular systems (OMS) have been widely used in the formation of mineral solids to control their composition, morphology, and dimensions. In this paper, we synthesized tricalcium phosphate by mixing two microemulsions, one containing calcium in its aqueous phase, the other containing phosphate. The microemulsions were stabilized either with the nonionic surfactant, Brij 30, or with the ionic surfactant, AOT, in *n*-decane. In the presence of Brij 30, the amorphous tricalcium phosphate gel formed was composed of spherical clusters and its crystallization into apatite used a process comparable to that observed in aqueous or water–alcohol medium. In contrast, the presence of AOT induced the production of a directly crystallized solid containing organic material, which could be due to AOT molecule preorganization at the oil–water interface. The growth of crystallites occurred in a preferential direction, and the crystals obtained were analogous in shape and size to particles of bone mineral. We develop the hypothesis of oriented apatitic nucleation on the organized AOT molecule support.

## Introduction

The mineral part of calcified tissues (bone, teeth) consists of calcium phosphates with an apatitic structure. They belong to a family of isomorphous compounds which crystallize in the hexagonal system and have the general formula:



with  $0 \leq x < 2$ .

In this family, two compounds hold a particular position, hydroxyapatite ( $x = 0$ ) and tricalcium phosphate ( $x = 1$ ). Hydroxyapatite (HAP), with an atomic Ca/P ratio of 1.67, is biocompatible and only slightly bioresorbable because of its insolubility. These properties, associated with those of osteoconduction, have led to it being used as a covering for prostheses. Apatitic tricalcium phosphate (TCP), with an atomic Ca/P ratio of 1.50, is also biocompatible but is more soluble than HAP; it is quickly biodegraded and replaced by neoformed bone.<sup>1</sup>

In living organisms, the synthesis of calcified tissue involves a process where the mineral–organic interface plays an essential part. The organic part conditions the composition and the structure of the solids, probably because of the existence of hybrid mineral–organic compounds at the interface. Bone tissue in particular is immersed in a liquid composed of water, lipids, and phospholipids (phosphoric diesters). An important role has been attributed to phospholipids

during calcification.<sup>2–5</sup> They are surfactants, interface molecules able to stabilize emulsions. Surfactants have been widely used in the formation of mineral solids in organized molecular systems (OMS):  $\text{CaCO}_3$ ,<sup>6</sup>  $\text{BaSO}_4$ ,<sup>7,8</sup>  $\text{CdS}$ ,  $\text{AgS}$ ,<sup>9,10</sup>  $\text{NH}_4\text{MnF}_3$ ,<sup>11</sup> etc. Some studies have been devoted to the synthesis of calcium phosphates in OMS using surfactants. For example, Murray<sup>12</sup> added an apatitic phosphate precipitated in aqueous medium to an emulsion composed of vegetable oil and nonionic surfactant and obtained hydroxyapatite with better mechanical holding than a powder obtained only in aqueous medium. Mann<sup>13</sup> prepared highly reticulated macroporous calcium phosphates from bicontinuous microemulsions. Recent works<sup>14,15</sup> deal with the synthesis of apatite by adding aqueous solutions of phosphate to emulsions or microemulsions of nonionic surfactant containing calcium in the aqueous phase.

(2) Irving, J. T. *Clin. Orthop.* **1973**, *97*, 225–236.

(3) Rabinowitz, J. L.; Tavares, C. J.; Lipson, R.; Person, P. *Biol. Bull.* **1976**, *150*, 69–79.

(4) Vogel, J. J.; Boyan-Salyers, B. D. *Clin. Orthop.* **1976**, *118*, 230–241.

(5) Wuthier, R. E. *Clin. Orthop.* **1973**, *90*, 191–200.

(6) Mann, S.; Heywood, B. R.; Rajam, S.; Birchall, J. D. *Nature (London)* **1988**, *334*, 692–695.

(7) Addadi, L.; Moradian, J.; Shay, E.; Maroudas, N. G.; Weiner, S. *Proc. Natl. Acad. Sci. U.S.A., Biophysics* **1987**, *84*, 2732–2736.

(8) Hopwood, J. D.; Mann, S. *Chem. Mater.* **1997**, *9* (8), 1819–1828.

(9) Pileni, M. P. *J. Phys. Chem.* **1993**, *97*, 6961–6973.

(10) Pileni, M. P. *Langmuir* **1997**, *13*, 3266–32.

(11) Roth M.; Hempelmann R. *Chem. Mater.* **1998**, *10* (1), 78–82.

(12) Murray, M. G. S.; Ponton, C. B.; Marquis, P. M. *Bioceramics* **1992**, *5*, 15–22.

(13) Walsh, D.; Hopwood, J. D.; Mann, S. *Science* **1994**, *264*, 1574–78.

(14) Qi, L.; Ma, J.; Cheng, H.; Zhao, Z. *J. Mater. Sci. Lett.* **1997**, *16*, 1779–1781.

(15) Lim, G. K.; Wang, J.; Ng, S. C.; Gan, L. M. *Mater. Lett.* **1996**, *28*, 431–36.

\* Corresponding author. Telephone: 05-61-55-65-32. Fax: 05-61-55-60-85. E-mail: lebugle@cict.fr.

(1) Rey, C. *Biomaterials* **1990**, *11*, 13–15.

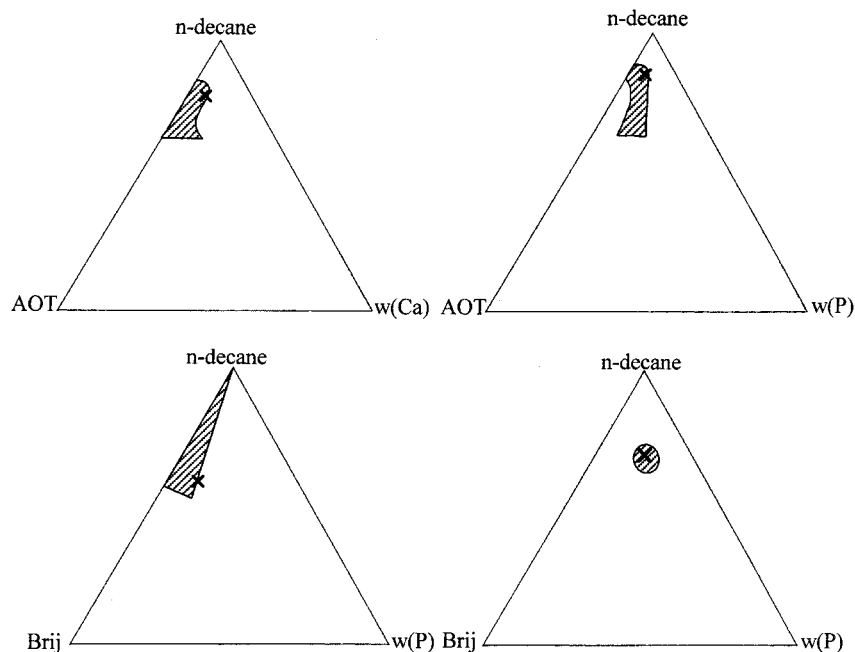


**Figure 1.** Phase diagrams of AOT/*n*-decane/aqueous phase and Brij 30/*n*-decane/aqueous phase at 25 °C. The shaded region shows the microemulsion domain; x, system studied.

In this paper, the synthesis used two microemulsions instead of only one, one containing calcium in the aqueous phase and the other containing phosphate. The droplets of the aqueous phase are restricted regions where the reactions occur under mild conditions, allowing the composition, morphology, and dimensions of the solids formed to be controlled, as shown by Pileni.<sup>9,10</sup> Also, during this study, we examined the influence of the type of surfactant (ionic or nonionic) on the formation of calcium phosphates. The two initial microemulsions were stabilized either with the nonionic surfactant, Brij 30 (polyoxyethylene-4-lauryl ether), or with the ionic surfactant, AOT (sodium dioctyl sulfosuccinate) in *n*-decane. We took particular interest in the synthesis of tricalcium phosphate which, as mentioned previously, has a key position in the apatite family.

### Experimental Section

Synthesis was performed by mixing two microemulsions, one containing calcium salt in the aqueous phase (W(Ca)), and the other containing phosphate (W(P)).

**Method.** The ternary phase diagrams of oil/AOT/water are well known.<sup>16,17</sup> However, the presence of a salt in the aqueous phase modifies the stable microemulsions domain. In this paper, it was necessary to specify the composition boundaries at which the oil/surfactant/aqueous phase microemulsion was transparent at 25 °C. The results are shown in Figure 1. The compositions studied are reported in Table 1.

The reagents were AOT (dioctyl sulfosuccinate sodium salt,  $\text{NaC}_{20}\text{H}_{37}\text{O}_7\text{S}$ , 99%, Aldrich), Brij 30 (polyethylene-4-lauryl ether,  $\text{C}_{12}\text{H}_{25}(\text{OCH}_2\text{CH}_2)_4\text{OH}$ , Aldrich), *n*-decane ( $\text{CH}_3(\text{CH}_2)_8\text{CH}_3$ , 99%, Aldrich),  $\text{Ca}(\text{NO}_3)_2 \cdot 4\text{H}_2\text{O}$  (Prolabo, for analysis), and  $(\text{NH}_4)_2\text{HPO}_4$  (Prolabo, for analysis). From these reagents, aqueous solutions of calcium and phosphate were prepared at 1 M and 0.5 M, respectively, and adjusted to pH ~9 with  $\text{NH}_4\text{OH}$  ( $d = 0.92$ ). These concentrations are within the microemulsion domain and yield enough powder for subsequent

**Table 1. Composition of the Microemulsions (Weight Percent)**

system	% oil	% surfactant	% aqueous phase
decane/Brij 30/w(Ca)	60	30	10
decane/Brij 30/w(P)	70	15	15
decane/AOT/w(Ca)	80	15	5
decane/AOT/w(P)	85	10	5

study. The aqueous calcium solution was filtered (Millipore, 0.2  $\mu\text{m}$ ) to remove traces of hydrated magnesium oxide precipitate which appears in basic medium (magnesium is indeed present as an impurity in the calcium salt, ~0.3% weight).

In this paper, obtaining precipitate with a (Ca/P)<sub>s</sub> (solid) atomic ratio of 1.5 (TCP) requires starting with a (Ca/P)<sub>r</sub> (reagent) atomic ratio in solution equal to 1.65 with a microemulsion stabilized by Brij 30, 2 with AOT. In both cases, the resulting  $w = [\text{H}_2\text{O}]/[\text{surfactant}]$  ratio was about 10: droplets were then small and few. The two calcium and phosphate microemulsions were prepared at ambient temperature and stored at 25 °C. They were then quickly mixed, manually shaken, and kept at 25 °C for an hour to a week, to study the effects of aging on the properties of the solid obtained. In the experiments with Brij 30, precipitation was immediate; the mixture obtained was thick, pearly, translucent and did not undergo noticeable precipitate decantation, even after a week. In those performed with AOT, precipitation was not immediate: the initially transparent mixture gained a pearly luster about half an hour later, whitened with aging, and sedimented from the first hour at 25 °C.

The precipitate was extracted from the reaction medium by centrifugation, washed three times in 95% ethanol (Brij 30 and AOT are soluble in ethanol) and then one last time with absolute ethanol to remove traces of water. Finally, it was dried under vacuum. A white powder was obtained. With Brij 30, about 1 g of the solid was obtained with 200 g of reaction mixture and about 0.2 g with AOT for a week. In the mixture, next to the precipitate, a microemulsion subsists, containing  $\text{NH}_4^+$  and  $\text{NO}_3^-$  counterions.

**Analysis Methods.** *Chemical Analysis.* The carbon, hydrogen, and sulfur levels were determined by elementary microanalysis on a Perkin-Elmer series B (model 2400). The relative errors were 0.3% weight for C, 0.2% for N, and 0.3% for S.

(16) Robinson, B. H.; Khan-Lodhi, A. N.; Towey, T. *Structure and Reactivity in Reverse Micelles*; Pileni, M. P., Ed.; Elsevier: New York, 1989; pp 198–220.

(17) Langevin, D. *Structure and Reactivity in Reverse Micelles*; Pileni, M. P., Ed.; Elsevier: New York, 1989; pp 13–43.

**Table 2. Molar Distribution per 100 g of Freeze-Dried Sample before Heating and Weight Loss**

surfactant	(Ca/P)r	duration	n(Ca) (mol)	n(PO <sub>4</sub> ) (mol)	n(C) (mol)	n(Na) (mol)	n(S) (mol)	(Ca/P)s	% weight loss (wt %)
Brij 30	1.65	1 h	0.84	0.56	0.20	0	0	1.50	22
		5 h	0.85	0.57	0.16	0	0	1.51	14
		7 d	0.89	0.59	0.20	0	0	1.51	13
AOT	2.0	1 h	0.66	0.44	0.72	0.07	0.03	1.50	28.0
		7 d	0.70	0.47	0.54	0.06	0.02	1.49	22.4

The presence of surfactants could disturb many titration reactions, so, in some cases, the samples were analyzed after heating to 900 °C under air and after dissolving in perchloric acid (calcium, phosphate, sodium titrations). The levels determined were corrected to represent those of the sample before heating, taking the weight loss observed during heating into account.

The level of sodium was measured with a specific electrode (ORION).

Calcium ion concentration was determined by volumetric titration,<sup>18</sup> and phosphorus by colorimetry as phosphovanadomolybdenum ( $\lambda = 460$  nm).<sup>19</sup> The relative error on the level of calcium and phosphate was 0.5%. The determination of the atomic Ca/P ratio of the precipitate had a relative error of 1%.

**FTIR.** FTIR analysis covered 400–4000 cm<sup>-1</sup> on a Perkin-Elmer FTIR 1600 spectrometer with pellets of 1 mg of sample and 300 mg of KBr.

**X-ray Diffraction (RDX).** The diagrams were obtained with a CPS 120 INEL diffractometer using the K $\alpha_1$  radiation of a cobalt anticathode ( $\lambda = 1.78892$  Å). The apparent crystallite size was calculated from (310) and (002) lines, applying Scherrer's formula:<sup>20</sup>

$$L_{(hkl)} = \frac{0.94\lambda}{(\cos \theta)\sqrt{\Delta_r^2 - \Delta_0^2}}$$

where 0.94 is the Scherrer constant;  $L$ , apparent size in the direction perpendicular to diffraction plane  $hkl$  (Å);  $\lambda$ , wavelength wave of X radiation ( $\lambda$  Co K $\alpha = 1.78892$  Å);  $\theta$ , diffraction angle corresponding to the  $hkl$  line considered;  $\Delta_r$ , width of the diffraction line of the sample (radian);  $\Delta_0$ , width of the same diffraction line of a well crystallized hydroxyapatite (radian). It was determined on a hydroxyapatite heated at 900 °C for 72 h. It was about 0.00128 rad for the (002) line and 0.00140 rad for the (310) line. Measurement accuracy from the (002) line was about 5 Å, whereas the (310) line gave only an estimation of the apparent size.

**Transmission Electron Microscopy (TEM).** The powders were observed in the TEMSCAN Electron Microscopy department of Paul Sabatier University (Toulouse) with a JEM-2010 microscope. Calcium phosphates tend to aggregate, so they were dispersed by ultrasound in absolute ethanol before observation.

## Results

**Chemical Analysis.** The results, shown in Table 2, are expressed in moles per 100 g of nonheated solid. Weight loss (weight percent of nonheated powder) observed after heating to 900 °C in air is also reported in this table.

The (Ca/P)s atomic ratio in freeze-dried samples was not dependent on aging times, it remained constant at about 1.50. The levels of carbon were low in the presence of Brij. They essentially result from carbonate ions present because of the basic pH of the aqueous solutions in the initial microemulsions. In the presence of AOT, the carbon levels were higher, this was partly due to the presence of carbonate, but mainly to AOT, as

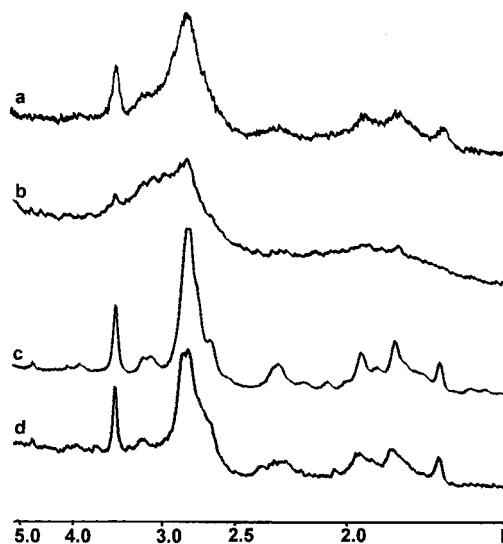


**Figure 2.** X-ray diagrams of (a) apatitic tricalcium phosphate prepared in aqueous medium dried at 80 °C; (b) powders prepared with Brij-30, for (Ca/P)r = 1.65 and 1 h of aging; (c) powders prepared with Brij-30, for (Ca/P)r = 1.65 and 5 h of aging; and (d) powders prepared with AOT, for (Ca/P)r = 2 and 1 h of aging.

indicated by the presence of sulfur from ionic surfactant head: 0.03 mol for an hour and 0.02 mol for a week.

Total weight loss, after heating to 900 °C under air essentially corresponds, when the surfactant was Brij 30, to water loss. When the solids were formed, they contained a high proportion of water which decreased notably during aging. A sample matured for 1 h at 25 °C presents about 22 wt % of water, which decreases to about 13 wt % a week, similar to the generally observed value for apatitic calcium phosphates. In the presence of AOT, weight loss by heating was essentially due to loss of surfactant (determined by elementary micro-analysis, the water level was deduced by difference) and to water loss.

**X-ray Diffraction.** The powders obtained with Brij 30 present diagrams characteristic of an amorphous product when maturation times were shorter than 5 h (Figure 2). Beyond, the spectra show broad lines characteristic of a poorly crystallized apatitic phosphate. On the other hand, the X-ray diagrams correspond to those of poorly crystallized apatite from the first stages of precipitation in systems with AOT.

Apparent crystallite size, calculated from (310) and (002) lines, are reported in Table 3. Crystal growth in direction (310) was much lower with AOT than with Brij 30. Then AOT blocked crystal development along a plane perpendicular to axis  $c$ .

It can be noticed that with AOT, the crystallites had a similar size to particles of bone mineral.<sup>21</sup>

**FTIR.** FTIR results confirm X-ray diagrams (Figure 3). With Brij 30, for maturation times shorter than 5 h,

(18) Charlot, G. *Masson, Paris* **1966**, 5, 658–659.

(19) Gee, A.; Deitz, V. R. *J. Am. Chem. Soc.* **1955**, 77, 2961–2965.

(20) Guinier, A. *Théorie et technique de la radiocristallographie*, 3rd ed.; Dunod Paris, **1960**.

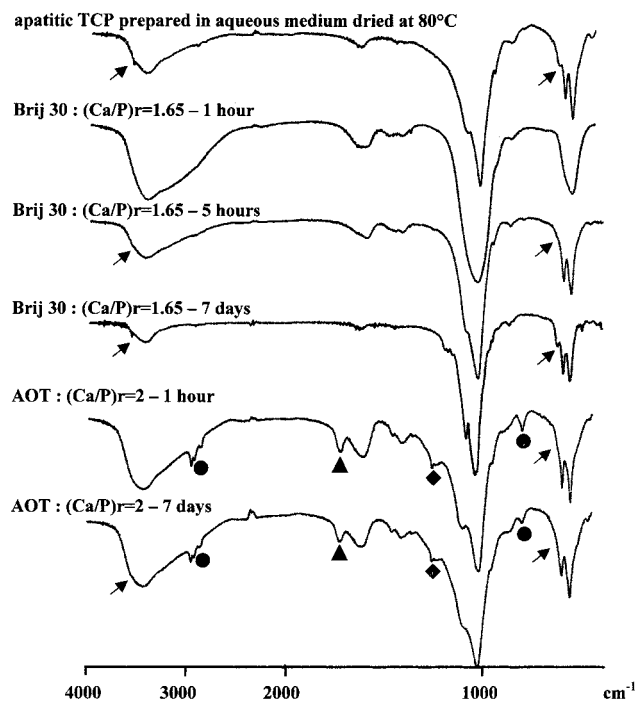


**Figure 3.** Infrared spectra of powder prepared in aqueous medium, in the presence of Brij 30 with  $(Ca/P)r = 1.65$ , and in the presence of AOT with  $(Ca/P)r = 2.0$ , with different times of aging: ●, C-H vibration bands; ▲, C=O vibration bands; ◆, O-S-O vibration bands; →, O-H vibration bands.

**Table 3. Variation of Apparent Crystallite Size along Lines (002) and (310), According to the Atomic (Ca/P)r Ratio, the Time of Ageing, and the Surfactant Used**

TA	(Ca/P)r	duration	L(002) (Å)	L(310) (Å)	L(002)/L(310)
Brij 30	1.65	5 h	203	90-100	~2.0
		7 d	265	90-100	~2.6
AOT	2.0	1 h	165	20-30	~6.0
		7 d	351	40-50	~12.0

solid spectra were those of an amorphous calcium phosphate. For longer times, the  $PO_4^{3-}$  bands at 600 and  $1000-1100\text{ cm}^{-1}$  can be seen to split, and OH<sup>-</sup> bands to appear at  $630$  and  $3560\text{ cm}^{-1}$ , and a  $HPO_4^{2-}$  band at  $875\text{ cm}^{-1}$ , characteristic of an apatitic environment. Weak bands at  $1384$  and  $1356\text{ cm}^{-1}$  are attributed to nitrate ions (which were not totally removed by washing) and at  $1421$  and  $1472\text{ cm}^{-1}$  to carbonate ions due to the basic pH of the initial aqueous solutions. On the other hand, organic material was only present in small amounts in the solids. With AOT, the spectra of freeze-dried samples are those of a straight apatitic calcium phosphate, regardless of the maturation time. The spectra also present bands attributed to nitrate and carbonate ions. On the other hand, many bands show the presence of organic material ( $2900\text{ cm}^{-1}$ ,  $1700-1600$ , and  $806\text{ cm}^{-1}$ ): AOT is therefore incorporated into the calcium phosphate prepared.

**Transmission Electron Microscopy (TEM).** Crystals obtained with Brij 30 appear in plates about 10 nm thick (Figure 4). Those obtained in the presence of AOT (Figure 5) are smaller than before ( $<10\text{ nm}$ ). These dimensions are in agreement with the values obtained from X-ray diffraction lines.



**Figure 4.** TEM micrograph of powder prepared in the presence of Brij-30 with  $(Ca/P)r = 1.65$  after 7 days of aging.

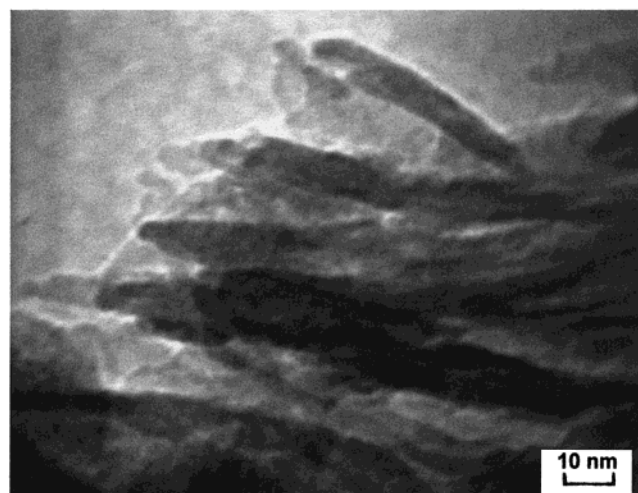


**Figure 5.** TEM micrograph of powder prepared in the presence of AOT with  $(Ca/P)r = 2.0$  after 7 days of aging.

## Discussion

The results show that apatite synthesis follows two different processes, depending on whether the surfactant used is ionic or not.

In the presence of Brij 30, a nonionic surfactant, phosphate precipitates were amorphous just after their formation and crystallized into apatite after a few hours of maturation. In parallel with this structural modification, their water content, about 22% weight after an hour, decreased and stabilized at about 13%. It can also be noticed that organic material was not bound to the solid and probably did not play any part in the crystallization process. So, formation of amorphous calcium phosphate gel and its crystallization into apatite uses a process comparable to that observed in aqueous and water-alcohol medium.<sup>22,23</sup> On precipitation, a gel rich in water was formed, composed of amorphous spherical clusters (Figure 6), as suggested by Betts and Posner.<sup>24</sup> Each cluster consists of an

(22) Rodrigues, A.; Lebugle, A. *Colloid Surf.* **1998**, *145* (1-3), 191-204.

(23) Heughebaert, J. C.; Montel, G. *Calcif. Tissue Int.* **1982**, *34*, S103-S108.

(24) Betts, F.; Posner, A. S. *Mater. Res. Bull.* **1974**, *9*, 353-360.

(21) Jackson, S. A.; Cartwright, A. S.; Lewis, D. *Calcif. Tissue Res.* **1978**, *25* (3), 217-222.

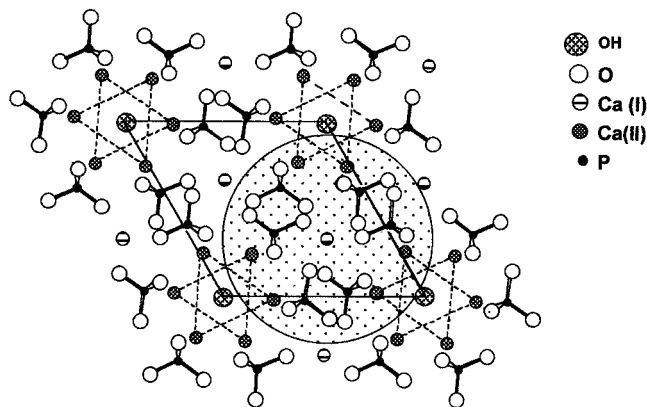


**Figure 6.** Projection on base plane (001) of the hydroxyapatite structure.<sup>28</sup> The circle shows the amorphous cluster corresponding to  $\text{Ca}_9(\text{PO}_4)_6$ , as suggested by Betts and Posner (ref 24).

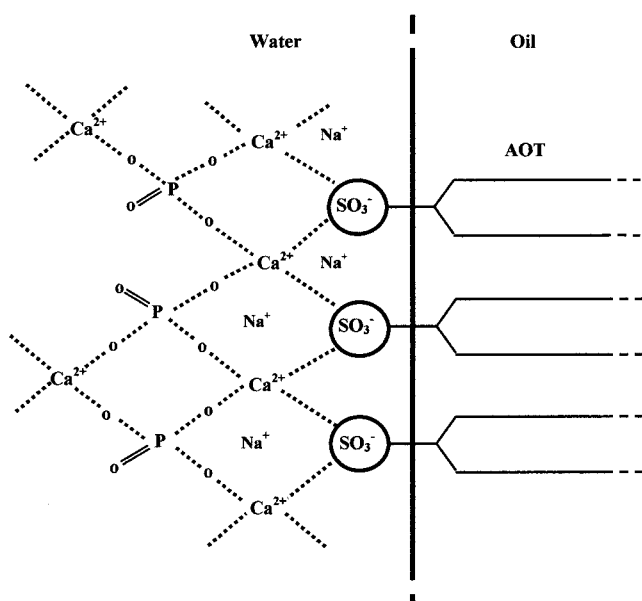


**Figure 7.** Model of oriented crystallization of calcium phosphate in the presence of AOT.

assembly of ordered microcrystallites of about 9.5 Å, containing nine  $\text{Ca}^{2+}$  ions and six  $\text{PO}_4^{3-}$  ions. Intercluster interstices are rich in water (10–20% weight).<sup>25</sup> During crystallization, the clusters migrate and join together to form aggregates. This association is accompanied by rearrangement of the Ca(II) ions which surround the apatite structure tunnels with elimination of most water of solvation. Various authors agree with this hypothesis.<sup>26,27</sup>

The calcium phosphates obtained in the presence of AOT were apatitic from the first stages of their precipitation and contained a large amount of organic material. The production of a directly crystallized solid could be due to AOT molecule preorganization at the oil/water (O/W) interface (Figure 7). Hydrophilic polar heads interact with water (H bonding) and long and ramified hydrophobic chains join up by van der Waals forces,

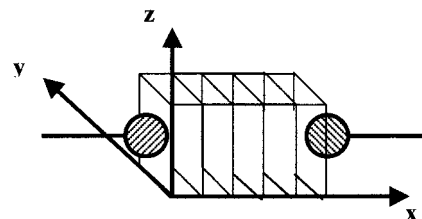
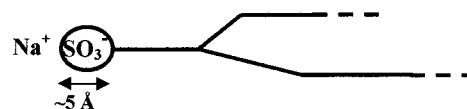


**Figure 8.** "Sandwich" model of apatite growth in the presence of AOT molecules.

#### AOT



#### Brij 30 :



**Figure 9.** Geometry of AOT<sup>32</sup> and Brij 30.

conferring the rigidity to the system. Because of their strong affinity for sulfonate ions,<sup>7</sup>  $\text{Ca}^{2+}$  ions are immobilized at the O/W interface and follow the geometry dictated by the association of surfactant molecule. During the addition of phosphate microemulsion, calcium ions bind simultaneously to the surfactant and to  $\text{PO}_4^{3-}$  ions. The outcome is oriented apatitic nucleation on the support composed of organized AOT molecules. Various authors have proposed the hypothesis that organized surfactant molecules lead to such inorganic crystal nucleation, particularly in the mechanism of formation of calcium carbonate like calcite<sup>7,29</sup> or aragonite observed in mollusc shells.<sup>30</sup>

The calculation of apparent crystallite size shows that growth occurs in a preferential direction parallel to axis *c*. Growth in a plane perpendicular to axis *c* is limited to about 10 Å, probably owing to the presence of strongly bound organic molecules. Chemical analysis indicated one AOT molecule per five or six apatite molecules, depending on aging. A "sandwich" model is therefore proposed, in which calcium phosphate grows perpendicularly to axis *c* and is limited to about five links (Figure 8).

The strong interaction between the  $\text{SO}_3^-$  ions of AOT with  $\text{Ca}^{2+}$  ions accounts for the observed results. Indeed, since the atomic surfactant/Ca ratio used in solution is high (about 5), calcium ions are likely to initially interact with sulfonate heads and will not immediately react with phosphate ions. This explains observed precipitation delay. By another route, the occurrence of this interaction can explain that part of the calcium ions remain sequestered and that the atomic (Ca/P)<sub>r</sub> ratio needed in solution (= 2) is distinctly higher than the value in the desired solid. When the surfactant was Brij 30, the interaction was insufficient to cause such phenomena, strongly reduced by the Brij hydrophilic heads, because of its weak ionic character (calculated from the difference of its atoms electronegativity, about 22%) and hydrophilic head geometry (Figure 9). The (Ca/P)<sub>r</sub> ratio necessary to obtain a solid with a (Ca/P)<sub>s</sub> equal

(25) Holmes, J. E.; Beebe, R. A. *Calcif. Tissue Res.* **1971**, *7*, 163–174.

(26) Harries, J. E.; Hukins, D. W. L.; Holt C.; S. S. Hasnain, J. *Crystal Growth* **1987**, *84*, 563–570.

(27) Grynopas, M. D.; Bonar, L. C.; Glimcher, M. J. *J. Mater. Sci.* **1984**, *19*, 723–736.

(28) Kay, M. I.; Young, R. A. *Nature* **1964**, *204* (4963), 1050–1052.

(29) Heywood, B. R.; Rajam, S.; Mann, S. *J. Chem. Soc., Faraday Trans.* **1991**, *87*, 727–734.

(30) Weiner, S.; Traub, W. *Proc. R. Soc. London, Ser. B* **1984**, *304*, 425–443.

to 1.50, was 1.65. This ratio was much greater than that observed in aqueous media,<sup>23</sup> it is close to the ratio used in water–alcohol media:<sup>31</sup> Brij 30, like ethanol, has the

---

(31) Zahidi, E.; Lebugle, A.; Bonel, G. *Bull. Soc. Chim. France* **1985**, *4*, 523–527.

(32) Huang, J. S.; Kotlarchyk, M. *J. Phys. Chem.* **1985**, *89*, 4382–4386.

property of decreasing the dielectric constant near the hydrophilic head. So, the precipitation was more complete.

Therefore systems stabilized by Brij 30 display a weak and nonorganized “mineral–organic” interface, whereas with AOT the interface is strong and well structured.

CM991022R